Макрогетероциклы
http://macroheterocycles.isuct.ru

DOI: 10.6060/mhc170830g

Crown– and Sulfophthalocyanines in Low–Molecular–Weight Hydrogels: Properties, Molecular State, and Release

N. F. Goldshleger,[a@1] A. S. Lobach,[a] N. N. Dremova,[a] M. A. Lapshina,[a] A. M. Kolesnikova,[a] V. E. Baulin,[b,c@2] and A. Yu. Tsivadze[b]

[a]*Institute of Problems of Chemical Physics RAS, 142432 Chernogolovka, Russia*
[b]*A.N. Frumkin Institute of Physical Chemistry and Electrochemistry RAS, 119071 Moscow, Russia*
[c]*Institute of Physiologically Active Compounds RAS, 142432 Chernogolovka, Russia*
[@1]*Corresponding author E-mail: nfgold@icp.ac.ru*
[@2]*Corresponding author E-mail: mager1988@gmail.com*

In continuation of our previous studies, we explored the solubilization of crown- and sulfophthalocyanines in the presence of bile salts (BS), sodium deoxycholate, and sodium taurodeoxycholate. The formation of BS-based low-molecular-weight hydrogels was observed and their modification with 15-crown-5-phthalocyanines was studied. Some characteristics of hybrid gels and xerogels are presented, and the process of prolonged release of active component from gel under the action of external stimuli was studied in detail.

Keywords: Metallophthalocyanines, crown ethers, biocompatibility, bile acid salts, solubilization, low-molecular-weight hydrogels, release, amino acids, absorption spectra.

Краун– и сульфофталоцианины как компоненты низкомолекулярных гидрогелей на основе солей желчных кислот: свойства, молекулярное состояние и высвобождение из геля

Н. Ф. Гольдшлегер,[a@] А. С. Лобач,[a] Н. Н. Дремова,[a] М. А. Лапшина,[a] А. М. Колесникова,[a] В. Е. Баулин,[b,c@] А. Ю. Цивадзе[b]

[a]*Институт проблем химической физики РАН, 142432 Черноголовка, Россия*
[b]*Институт физической химии и электрохимии им. А.Н. Фрумкина РАН, 119071 Москва, Россия*
[c]*Институт физиологически активных веществ РАН, 142432 Черноголовка, Россия*
[@1]*E-mail: nfgold@icp.ac.ru*
[@2]*E-mail: mager1988@gmail.com*

Изучена солюбилизация краун- и сульфофталоцианинов в присутствии солей желчных кислот (BS) – дезоксихолата натрия и тауродезоксихолата натрия. Показано образование низкомолекулярных гидрогелей на основе солей желчных кислот, изучена их модификация с участием краун-содержащих фталоцианинами. Приведены характеристики гибридных гелей, а также изучен процесс высвобождения активного компонента из геля при внешнем воздействии.

Ключевые слова: Металлофталоцианины, краун-эфиры, биосовместимость, соли желчных кислот, солюбилизация, низкомолекулярные гидрогели, высвобождение, аминокислоты, спектры поглощения.

Introduction

Gels attract a lot of attention because their abundance in nature and the wide use of gel-forming compositions for industrial and household purposes. As is known, labile supramolecular ensembles of low- and high-molecular-weight gelators can act as excellent hosts for incorporating various guests, including nanomaterials.[1-3] Supramolecular gels based on small molecules look advantageous for the following reasons. Apart from their amphiphilicity of molecules and participation of non-covalent interactions in the process of gelation (as in biological structures), they are characterized by accessibility, high purity, known chemical structure, biocompatibility of the initial components, and the process of their gelation is rather simple. In addition, these gels are sensitive to external influences such as temperature, p*H*, medium polarity, *etc.*[4-8]

Bile acid salts, along which sodium taurodeoxycholate and sodium deoxycholate, belong to the class of natural surfactants with clear-cut features. Their molecules have a rigid, slightly bent sterane frame. In contrast to conventional surfactants such as sodium dodecyl sulfate (Figure 1), steroid micelle-forming compounds exhibit planar diphilicity. The use of natural surfactants for solubilization of drugs affords for designing a biocompatible environment. The important role of bile salts in the assimilation and delivery of drugs was discussed in reviews.[9,10]

The solubilization of magnesium octa[(4'-benzo-15-crown-5)-oxy]phthalocyanine ($Mgcr_8Pc$) in micellar solutions of SDC[11] ensures the embedding of $Mgcr_8Pc$ (Figure 1) into supramolecular gels of SDC[12] at the values of p*H* and ionic strength close to environment-friendly physiological ones.

This work is aimed at: (a) extending the range of natural surfactants suitable for solubilization of crown-containing phthalocyanines and at exploring, (b) the behaviour of new Pc in low-molecular-weight hydrogels based on bile salts, and (c) a process of active component release from the gel. The properties of the systems under study were characterized by absorption spectroscopy, scanning electron microscopy, X-ray powder diffraction, Fourier transform infrared spectra, and fluorescence microscopy.

Experimental

General. The synthesis of magnesium and zinc octa[(4'-benzo-15-crown-5)oxy]phthalocyanines was carried out as described elsewhere.[13,14] Magnesium tetra[(4'-benzo-15-crown-5) oxy]phthalocyanine was also obtained as described in [13]. Commercially available sodium taurodeoxycholate and sodium deoxycholate (Aldrich, 98 %), nickel(II) phthalocyanine-tetrasulfonic acid tetrasodium salt (Aldrich), lysine hydrochloride (99 %), L-lysine (pharmacopeia grade, KhimMed), L-histidine (Aldrich), and NaCl (exra-pure grade) were used without further purification. All solutions were prepared by using twice-distilled water.

Aqueous solution of $Mgcr_8Pc$ (or $Zncr_8Pc$) of a known concentration was used as a stock solution. To $Mgcr_8Pc$ solution, the weighed amounts of lys·HCl, SDC, and (if needed) NaCl were added successively. Monitoring was continued until attaining a constant optical density. The solutions were stored in the dark.

Deposition of coatings. 0.3 ml of $Mgcr_8Pc$/SDC/lys·HCl or SDC/lys·HCl solution was applied onto a 2 cm^2 silica plate just after recording the absorption spectrum. The concentration of $Mgcr_8Pc$, SDC, and lys·HCl had a value of $1.42 \cdot 10^{-5}$, 0.0264, and 0.124 M, respectively. The time allowed for gel formation was around 15 min, after which the samples were dried in the dark at room temperature. Thus, the prepared samples contained about $4.26 \cdot 10^{-9}$ mol of $Mgcr_8Pc$. Other samples were prepared in a similar way.

Absorption spectra of solutions and gels were recorded with a Specord M-40 spectrophotometer (with a thermostatted sample compartment) linked to a PC (for data acquisition) by using 1-, 2-, and 10-mm quartz cells or 0.02 mm layer clammed between two silica plates, respectively. In some cases, the absorption spectra were deconvoluted by using program package Origin.

IR spectra of individual compounds and gels in the range 4000–675 cm^{-1} were taken with a Perkin Elmer Spectrum 100 Fourier spectrometer equipped with a UATR accessory (Ge crystal).

Fluorescence microscopy. A required amount of gel or solution was applied onto a carefully processed and dried microscope slide. Solution samples were dried in a closed volume at room temperature and then protected by a cover glass. The images taken with an Axio Scope.A1 microscope (Carl Zeiss, Germany) were visualized by using a high-resolution camera AxioCam MRc 5 with an A-Plan 40x/0.65 M27 lens (WD=0.45 mm) and a set of glass filters 45 HQ Texas Red (E), d=25, EX BP 560/40, BS FT 585, EM BP 630/75. The images were processed by using ZEN 2012 (blue edition) software developed for an Axio Scope.A1 microscope (Carl Zeiss, Germany).

SEM measurements. The samples of xero- and aerogels were prepared by casting solutions onto a Si or Si/SiO_2 substrate followed

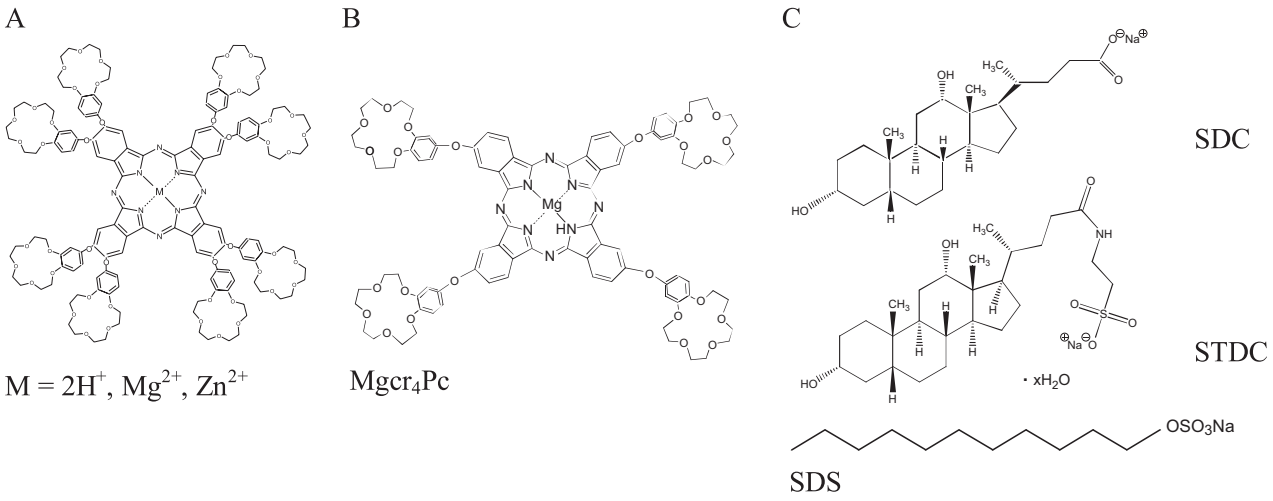

Figure. 1. A, B: Crown-containing phthalocyaninates; C: sodium deoxycholate, sodium taurodeoxycholate, and sodium dodecyl sulphate (see footnotes for abbreviations).

by in-air or lyophilic drying, respectively. In experiments we used a Supra 25 Zeiss microscope with the Schottky cathode and in-lens detector of secondary electrons (E_e=3–4 kV, P=2·10^{-4} Pa). In some cases, the conductivity was increased by the deposition of a carbon layer onto the sample surface. Elemental composition (at. %) of crystals in Mgcr$_8$Pc/SDC/NaCl aerogel was determined by energy dispersive X-ray (EDX) spectroscopy. Found: C 52.48, O 5.71, Na 19.65, Cl 22.17. For composition: SDC/8NaCl (24C+4O+9Na+8Cl, hydrogen neglected), calculated: C 53.33, O 8.8, Na 20, Cl 17.77.

X-Ray diffraction. Diffraction patterns were taken and processed by using an ADP-2-01 diffractometer (Cu-Kα radiation, Ni filter), the X-RAY software developed for DRON diffractometers, and JCPDS databases PDF-1 (sets 1–32) and ICDD 1995 (sets 1–45).

Results and Discussion

In this work, two bile salts − SDC and STDC − were used as gelators. For crown-containing phthalocyaninates, Mcr$_x$Pc (M=Mg, Zn, x=8 and M=Mg, x=4), and nickel tetrasulfophthalocyanine, NiPc(SO$_3$Na)$_4$, used as guest molecules, the information on the molecular state of Pc and its environment was derived largely from their optical absorption spectra. The latter ones afford for the estimation of extinction coefficient ε (M^{-1}·cm^{-1}) and other important parameters.

Zncr$_8$Pc and Mgcr$_8$Pc

Just as Mgcr$_8$Pc,[11] Zncr$_8$Pc solubilizes in micellar solutions of SDC. The absorption spectra reveal a high degree of Zncr$_8$Pc aggregation at the Pc concentration around 5.6·10^{-6} M. With increasing ionic strength of solution (addition of NaCl), the extent of Pc aggregation diminishes.

Although the absorption spectra of Mgcr$_8$Pc and Zncr$_8$Pc micellar SDC solutions containing NaCl are rather similar, the aggregation of Zncr$_8$Pc looks more pronounced. In the Zncr$_8$Pc/SDC/lys·HCl/NaCl system, the process of gel formation proceeded similarly to that in the Mgcr$_8$Pc/SDC/lys·HCl/NaCl system; in other words, the replacement of metal ion in the macrocycle of (Mg by Zn) had little or no influence on the process of gelation yielding dense gel. The process is accompanied by spectral changes and a decrease in the intensity of the *Q*-band. The absorption spectrum of Zncr$_8$Pc monomer restored upon gel melting.

An increase in the surfactant concentration of Mgcr$_8$Pc/STDC system is accompanied by an increase in the absorbance that continues to grow after the addition of NaCl, just as it was observed for SDC. On the other hand, the optical density of Mgcr$_8$Pc/STDC/NaCl solution was found to decrease upon the addition of lys·HCl ([lys·HCl] > [STDC]), just as in the case of Mgcr$_8$Pc in the presence of cationic surfactant.[15] Although the behaviour of Mgcr$_8$Pc in micellar solutions of SDC and STDC is rather similar, and the mechanical strength of SDC gel grew upon the addition of lys·HCl and NaCl, the STDC gel did not form under similar conditions. Upon heating the microheterogeneous Mgcr$_8$Pc/STDC/NaCl system, the intensity of the *Q*-band increased insignificantly.

Mgcr$_4$Pc

Influence of the number of crown-containing substituents introduced into the macrocycle through the oxygen bridge on the process of Pc solubilization in water was studied previously.[15] In contrast to Mcr$_8$Pc (M=Mg, Zn), Mgcr$_4$Pc not only is insoluble in water, but also is poorly solubilized by bioorganic surfactants, STDC and SDC. As follows from Figure 2 (spectrum 1), Mgcr$_4$Pc becomes soluble (largely in its aggregated state) only after sonication. The addition of NaCl in nearly physiological concentrations increases the extent of Pc encapsulation into micelles (Figure 2, spectrum 2). The solubilizing ability of the systems STDC and STDC/NaCl ([surfactant] >> CMC, critical micelle concentration) towards Mgcr$_4$Pc was about 20 and 56 % (after centrifuging and SDS addition), respectively. After centrifuging, the absorption spectra of the above microheterogeneous systems, e.g. Mgcr$_4$Pc/STDC/NaCl, exhibited the presence of monomer and Pc aggregates. Deconvolution of the recorded spectrum into the constituent Gaussian functions (R^2=0.9995) has shown that the fraction of aggregated particles (λ_{max}=671 nm and 751 nm) is markedly higher than that of monomeric ones (λ_{max}=651 nm and 688 nm). In Figure 2 spectrum 3 corresponds to the absorption of monomeric Mgcr$_4$Pc in micellar solution of a traditional anionic SDS. Note also that the absorption spectra of Mgcr$_4$Pc/STDC/NaCl and Mgcr$_8$Pc/STDC/NaCl markedly differ from those of Pc in micellar SDS solution.

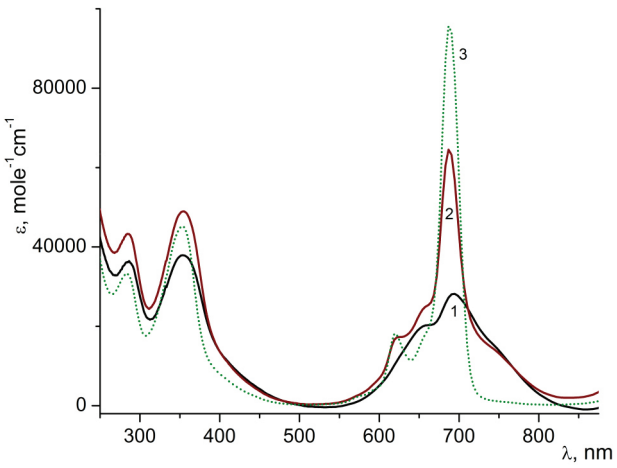

Figure 2. Absorption spectra of Mgcr$_4$Pc/STDC micellar solution centrifuged before (1) and after addition of NaCl (2): [Mgcr$_4$Pc]=3.42·10^{-5} M, [STDC]=0.0147 M, [NaCl]=0.29 M; and absorption spectrum of Mgcr$_4$Pc/SDS micellar solution (3): [Mgcr$_4$Pc]=1.07·10^{-4} M, [SDS]=0.0136 M.

Mgcr$_4$Pc/gel

Since no gelation was observed for the Mgcr$_8$Pc/STDC/NaCl/lys·HCl system, in this case the gelating system had the composition STDC/SDC/NaCl/lys·HCl. At low NaCl concentration (0.018 M), the system was in the state of viscous liquid. Upon an increase in [NaCl] and after repeated heating–cooling cycles, the system acquired the state of 'strong' gel (lower photo in Figure 3A). At room temperature, Mgcr$_4$Pc in gel can be assumed to exist largely in the form of the Pc aggregates associated with micelles.

Heat-induced gel → solution transition gives rise to growth in the intensity of the *Q*-band peaked at 685 nm

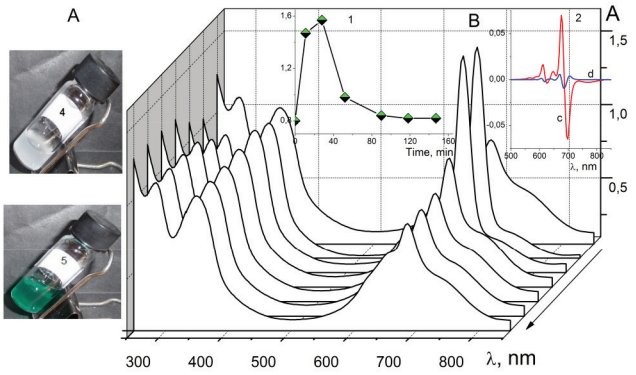

Figure 3. A: Photos of STDC/SDC/NaCl/lys·HCl (up) and $Mgcr_4Pc$/STDC/SDC/NaCl/lys·HCl gels (down). B: Absorption spectra of the $Mgcr_4Pc$/STDC/SDC/NaCl/lys·HCl system [gel−solution (melt)−gel]: $[Mgcr_4Pc]=1.25\cdot10^{-5}$ M, [SDC]=0.0118 M, [lys·HCl]=0.2 M, [NaCl]=0.1 M, and [STDC]=0.0018 M. In insert 1: Absorbance change caused by gel → solution (melt) → gel phase transformations during temperature rise up to 55 °C and subsequent cooling down to room temperature. In insert 2: the first (c) and second (d) derivatives of the $Mgcr_4Pc$ spectrum of gel melt, in which Pc is largely present as a monomer.

(Figure 3B). This is indicative of releasing $Mgcr_4Pc$ monomer in its micelle-bound form (log ε=5.08), just as in case of $Mgcr_8Pc$. Absorbance change caused by gel → solution (melt) → gel phase transformations during temperature rise up to 55 °C and subsequent cooling down to room temperature is illustrated in insert 1 to Figure 3B.

Nickel phthalocyanine tetrasulfonate

Figure 4 represents the absorption spectra of nickel phthalocyanine tetrasulfonate, $(NiPc(SO_3Na)_4$, in various media. In 50-% ethanol, $NiPc(SO_3Na)_4$ is present in its monomeric form (log ε=5.06, A_{668}/A_{602}=3.28, spectrum 1). The addition of SDC leads to the weakening and broadening

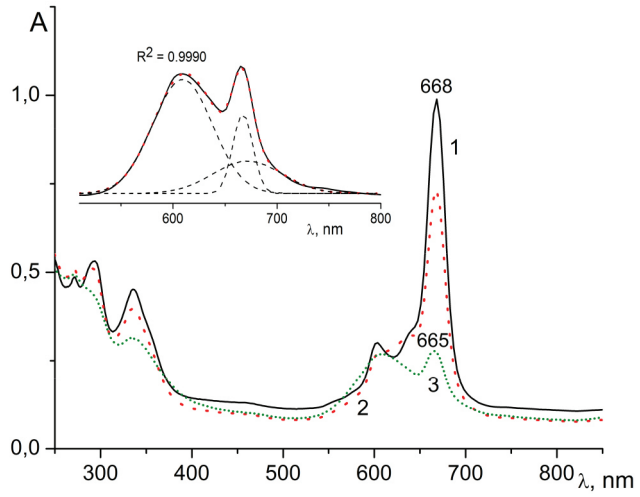

Figure 4. Absorption spectra of nickel tetrasulfophthalocyaninate ($[NiPc(SO_3Na)_4]=8.72\cdot10^{-6}$ M) in 50-% ethanol: (1) without additives; (2) at [SDC]=0.016 M (2); and (3) at [SDC]=0.016 M, [NaCl]=0.154 M. In the insert: spectrum 3 (solid line) and its deconvolution into three Gaussian functions (R^2=0.9990).

of the *Q*-band (A_{668}/A_{602}=2.63, spectrum 2). The process goes further upon the addition of NaCl (spectrum 3), and the band at 668 nm gets shifted to 665 nm. The overall appearance of the spectrum and the ratio $A_{665}/A_{602}\approx1$ (see insert of Figure 4) suggest the predominance of Pc aggregation. Prolonged storage resulted in insignificant spectral changes, but no gelation was observed.

The state of $NiPc(SO_3Na)_4$ in the above systems is defined by the following factors: 1) anionic surfactants have little or no influence on the state of anionic Pc; 2) at 303.15 K, critical micelle concentrations for SDC in water and aqueous ethanol (0.1 and 0.2 v/v) are 2.91, 3.74, and 4.15 mM, respectively.[16] The above increase in CMC with the volume fraction of ethanol is not in contradiction with the absence of micellization of sodium cholate and SDC in 1:1 and 1:2 water–ethanol mixtures (see[17] and references in). Together with an increase in the ionic strength caused by the addition of NaCl and the absence of coordinated axial ligands, the above said promotes the aggregation of $NiPc(SO_3Na)_4$.

In absorption spectrum 1 ($NiPc(SO_3Na)_4$ in water, Figure 5), the A_{625}/A_{663} ratio is around 1.46. Upon successive addition of SDC and NaCl, the long-wavelength shoulder shifts (see spectrum 2 in Figure 5) from 663 to 671 nm. At this, the ratio of band intensities changes from A_{625}/A_{663}=1.46 $[NiPc(SO_3Na)_4]$ *via* A_{625}/A_{671}=1.065 $[(NiPc(SO_3Na)_4$/SDC] to A_{621}/A_{671}=1.24 $[NiPc(SO_3Na)_4$/SDC/NaCl]. The addition of lys·HCl to the $NiPc(SO_3Na)_4$/SDC/NaCl system facilitated the formation of the gel whose absorption spectra were close to that of aqueous $NiPc(SO_3Na)_4$ solution (largely H-dimers and the *Q*-band shifted from 625 to 615 nm).

Characterization of gels

Absorption spectra. The *Q*-band in the absorption spectra of hybrid $Mgcr_8Pc$-containing gels represents the superposition of two strong and broad bands (spectra 1–3 in Figure 6c). The band peaked at 685 nm is assigned to monomeric $Mgcr_8Pc$, as follows from comparison with the spectrum of $Mgcr_8Pc$ micellar solution in SDC/NaCl (spectrum 4 in Figure 6c) while the short-wave band,

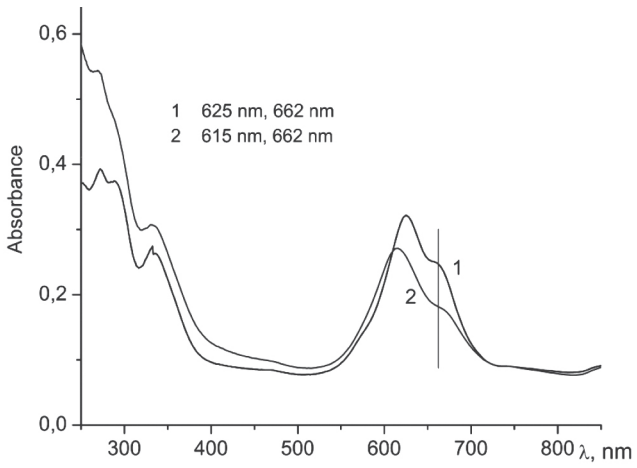

Figure 5. Absorption spectra of aqueous $NiPc(SO_3Na)_4$ solution (1) and $NiPc(SO_3Na)_4$/SDC/NaCl/lys·HCl gel (2): $[NiPc(SO_3Na)_4]=7.36\cdot10^{-6}$ M, [SDC]=0.0252 M, [NaCl]=0.18 M, and [lys·HCl]=0.142 M.

to the aggregated particles. In the presence of lys·HCl, the low-energy component becomes red-shifted (spectra 1 and 2). Comparative analysis suggests that the degree of Pc aggregation in gels decreases in the presence of NaCl and this is accompanied by the intensification of absorption at 685 nm, just as it was observed in solution.[11]

A difference in the state of $Mgcr_8Pc$ in $Mgcr_8Pc$/SDC/lys·HCl/NaCl and $Mgcr_8Pc$/SDC/NaCl hydrogels can be seen by comparing their spectra in Figure 6 with that of the $Mgcr_8Pc$ film (insert to Figure 6) obtained by drying in air.[18] For the former ones, the A_{685}/A_{643} ratio is around 1.6 while for the latter, $A_{698}/A_{643}\approx0.82$ and the long-wavelength shoulder is red-shifted. In the deconvolution, the fraction of $Mgcr_8Pc$ monomer (surface area under the peak with λ_{max}=686 nm) made a value of 42–44 and 22–25 % in $Mgcr_8Pc$/SDC/lys·HCl/NaCl and $Mgcr_8Pc$/SDC/NaCl gels and their xerogels, respectively. This implies that, upon drying, some certain number of $Mgcr_8Pc$ molecules is retained in the SDC or SDC/NaCl surrounding.

This was also confirmed by the fluorescence micrographs. As an example, Figures 7b and 7c present the fluorescence micrographs of $Mgcr_8Pc$/SDC/lys·HCl/NaCl gel and $Mgcr_8Pc$/SDC/NaCl xerogel. Bright red areas

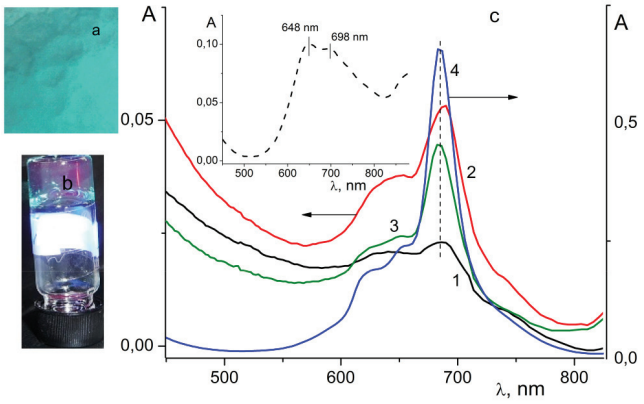

Figure 6. Photos of $Mgcr_8Pc$/SDC/lys·HCl/NaCl gel (a) and $Mgcr_8Pc$/SDC/lys·HCl gel (b) under illumination in the near-UV spectral range;[19] c: absorption spectra of $Mgcr_8Pc$/SDC/lys·HCl (1), $Mgcr_8Pc$/SDC/lys·HCl/NaCl (2), $Mgcr_8Pc$/SDC/NaCl gels (3) and of micellar solution of $Mgcr_8Pc$/SDC/NaCl (4). Quartz slide was used as a substrate. For all gels, the [SDC]/[$Mgcr_8Pc$] ratio was around 790. In the insert: absorption spectrum of $Mgcr_8Pc$ film.

can be attributed to the fluorescence of supramolecular aggregates with Pc. Since in our conditions the fluorescence of H-aggregated Pc is quenched,[20] Pc may be assumed to be partly present in its molecular state.

IR spectra. FTIR-ATR spectra of the gels under consideration and of their components are presented in Figure 8. Initially, the spectrum of $Mgcr_8Pc$/SDC/NaCl gel (Figure 8A) showed only the presence of water, but as the evaporation progressed, the bands of SDC came out more and more pronounced. As compared with individual compounds, all bands turn broadened. The vibration modes of C–H bonds in SDC were practically the same as those in SDC (curves 2 and 3 in Figure 8B). In the spectra of SDC and its gels, the bands peaked at 1560, 1408, and 1042 cm^{-1} was assigned to the vibrational modes of DC− and C–O bond of secondary alcohol in SDC, respectively. Since in the spectrum of $Mgcr_8Pc$/SDC/NaCl gel (curve 3 in Figure 8B) the characteristic modes of Pc (curve 1 in Figure 8B) are practically absent (because of excessive amount of SDC: SDC/$Mgcr_8Pc\approx800$), the presence of $Mgcr_8Pc$ is evidenced by electronic absorption (*cf.* Figure 6c). Meanwhile, the IR spectrum of Mgcr8Pc/SDC/NaCl gel exhibits a weak band at 1706 cm^{-1} (see Figure 8A and insert to Figure 8B). Thus, the band peaked at 1704 cm^{-1} was attributed to the –C=O stretching mode of –COOH group in deoxycholic acid.[21]

XRD results. The relevant diffraction patterns are collected in Figure 9. XRD patterns 1 and 2 in Figure 9A reveal no reflexes from SDC. The amorphism of SDC powder was reported in the literature.[22,23] In case of SDC xerogel, the halo located in the range 2θ=8.5÷35° with maxima 14.55 and 21.00° (d=6.088 and 4.230 Å, respectively) is observed. The halo of SDC powder is within the same range and peaked at 20.55°. The diffraction spectra of SDC xerogel, SDC powder, and $Mgcr_8Pc$/SDC/NaCl xerogel are similar. However, the latter exhibits (curve 3 in Figure 9A) the peaks belonging to NaCl crystals, which correspond to reflections from (111), (200), (220), (222), (400), and (420) planes (d=3.255, 2.818, 1.627, 1.469, and 1.261 Å).[24] The presence of NaCl crystals in SDC/NaCl dried gel was also reported in [25].

The spectra of crystalline lys·HCl powder and SDC/lys·HCl xerogel (SDC/lys·HCl≈1:1) are given in Figure 9B. For the latter, no structural features are noted, except for weak signals from lys·HCl and, probably, SDC, along with a shift of halo toward larger diffraction angles, as compared to SDC (see Figure 9A).

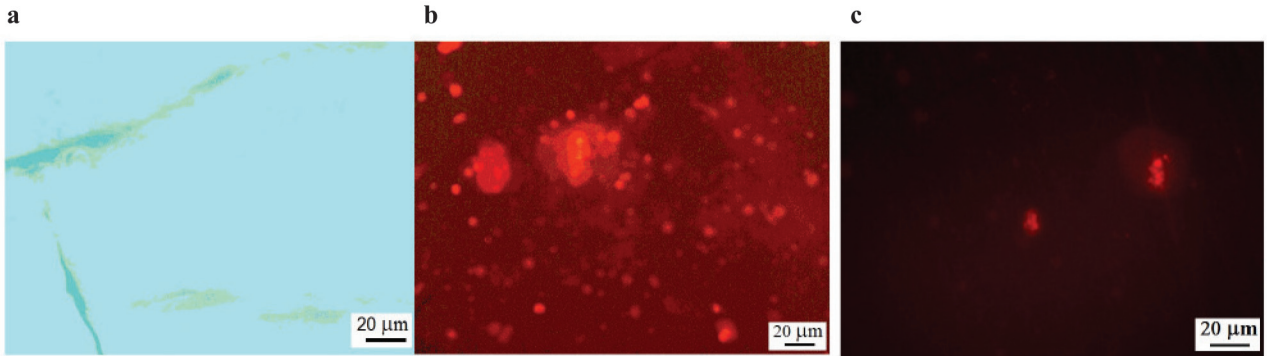

Figure 7. Micrographs of $Mgcr_8Pc$/SDC/lys·HCl/NaCl gel: no excitation (a), in fluorescence (b); of $Mgcr_8Pc$/SDC/NaCl xerogel in fluorescence (c).

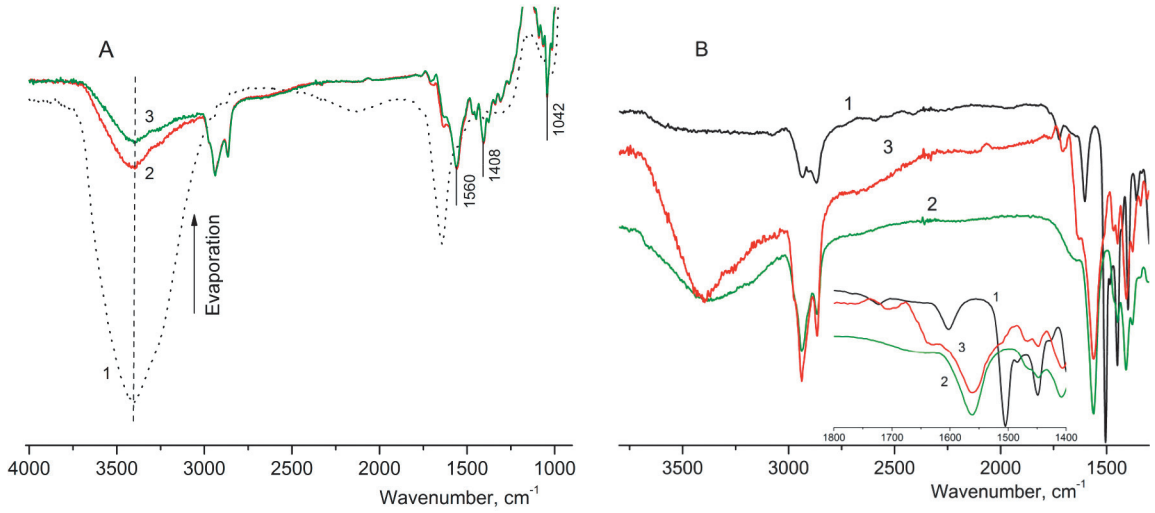

Figure 8. FTIR spectra of: (A) $Mgcr_8Pc$/SDC/NaCl gel taken in the course of drying its micro droplet on a Ge crystal; and (B) $Mgcr_8Pc$ (1), sodium deoxycholate (2), and $Mgcr_8Pc$/SDC/NaCl xerogel (3). In the insert: vibrational modes of DC^- and possibly –C=O group in deoxycholic acid.

The amorphous state of the above samples indicates the formation of SDC-based supramolecular gel *via* hydrogen bonds and/or Na^+ cations. With increasing crystallinity of modified SDC-containing gel, the diffraction patterns exhibited the appearance of peaks at 31.3 and 45.4°.[26]

SEM results. Selected examples of SEM images are presented in Figures 10 and 11. The surface of freeze-dried SDC/lys·HCl gel (Figures 10a,b) is seen to have a spongy structure with a partition thickness of 200–300 nm. Another situation is observed for $Mgcr_8Pc$/SDC/lys·HCl/NaCl gel with a deposited carbon coating: in this case, the nanofibers acquired a helical shape (Figure 10c).

The morphology of $Mgcr_8Pc$/SDC/NaCl xerogel is illustrated in Figure 11a. Its layered structure is seen to contain pores 200–500 nm in size and some crystalline inclusions. Meanwhile $Mgcr_8Pc$/SDC/NaCl aerogel (Figure 11d) represents the 3D network of entangled fibers 2–5 μm in diameter and dozen μm long. At larger magnification (Figure 11e), we can see that the fibers consist of rod-like aggregates around 1 μm long and 100–200 nm wide, along with white branched dendritic crystals (Figure 11e). The EDX analysis has shown that their elemental composition corresponds to a supramolecular structure formed with the involvement of SDC and enriched with NaCl (Figure 12). The latter is in line with the presence of NaCl peaks in the diffraction pattern (*cf.* Figure 9A). Earlier,[25] the formation of self-assembled aggregates of nanorods was observed in the system 50 mM SDC/30 mM alanine/100 mM NaCl.

Release of $Zncr_8Pc$ from gel. Upon addition of lysine solution to an aged $Zncr_8Pc$/SDC/lys·HCl/NaCl gel, we observed a gradual decrease in the height of gel column and concomitant increase in the intensity of the *Q*-band (Figure 13). This implies that the dissolution of gel and the release of Pc take place at room temperature.

Note that the presence of lysine produces little or no influence on the shape and position of the *Q*-band maximum as compared with $Zncr_8Pc$/SDC/NaCl micellar solution.

In the absence of lysine, *i.e.* upon the release of Pc from the gel under the action of water, the optical density (A_{685}) reached its maximum value and levelled-off

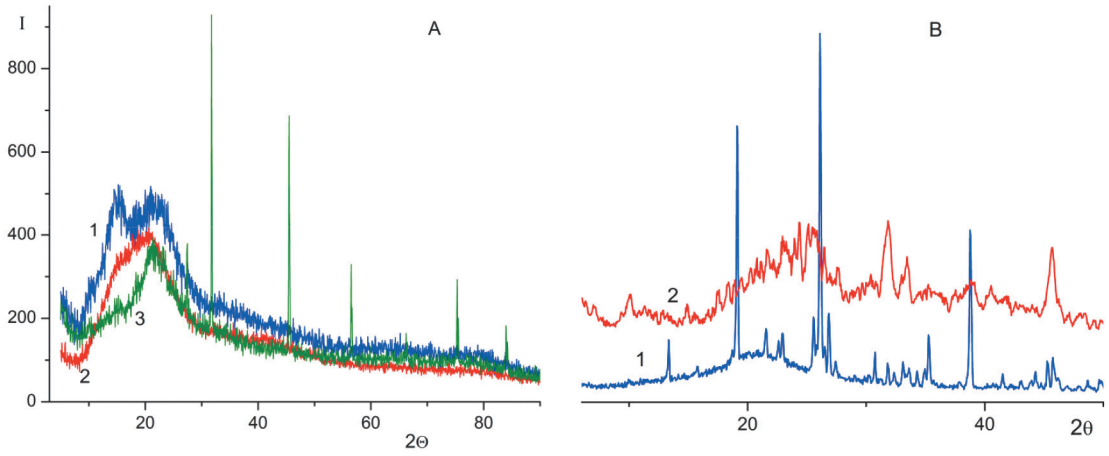

Figure 9. (A) XRD patterns of SDC xerogel (1), SDC powder (2), and $Mgcr_8Pc$/SDC/NaCl xerogel (3); and (B) XRD patterns of crystalline lys·HCl (1) and SDC/lys·HCl xerogel (2).

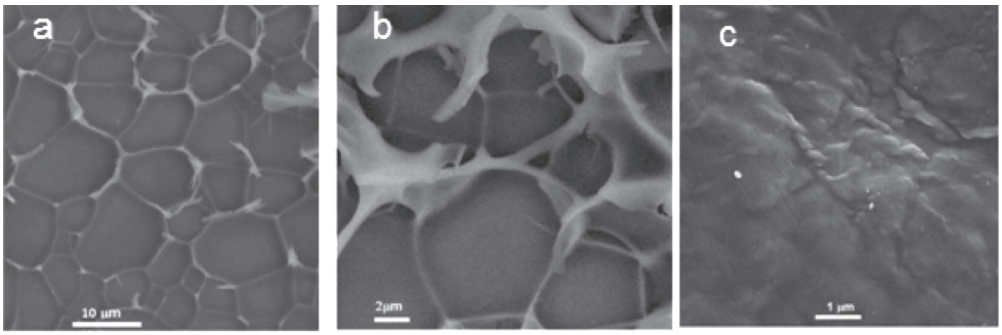

Figure 10. SEM images of: (a, b) freeze-dried SDC/lys·HCl gel and (c) $Mgcr_8Pc$/SDC/lys·HCl/NaCl gel with carbon coating.

(Figure 14b). During this time period, the gel did not dissolve but slightly grew in its volume. In Figure 14a, the cell is turned upside down at some time moment within the ascending part of the plot in Figure 14b, so that the aqueous solution here is below whereas the gel column, above. The greenish colour of the aqueous phase clearly evidences the transfer of Pc from gel to solution. A ratio of first-order rate constants for the release of Pc from gel in the presence of lysine to that from water was found to be around 4 for over a time period required for complete dissolution of $Zncr_8Pc$/SDC/lys·HCl/NaCl gel.[27]

In the presence of histidine (hydropathy index –3.5),[28] $Zncr_8Pc$/SDC/lys·HCl/NaCl gel remained undissolved for 24 h, but the transfer of Pc to the aqueous phase did occur. The absorption spectra indicate the presence of Pc in its different states, including the monomeric one. The latter can be tentatively explained by the transfer of SDC and NaCl in the amounts sufficient for monomerization of $Zncr_8Pc$. Upon prolonged storage under scattered illumination, we observed the photobleaching of Pc, without emergence of new absorption bands in the visible (true photobleaching). Similar behaviour was observed for Pc with four fused crown fragments[29] and for Pc with eight methyl phosphonate groups.[30]

Supramolecular organization of $Mgcr_xPc$ in hydrogels

Bile salts are anionic natural surfactants that can act in aqueous media as low-molecular-weight gelators (see[31] and references in). The formation of clusters − primary and secondary prolate SDC micelles − followed by the formation of markedly larger aggregates in the form of nanofibers and subsequent gelation was demonstrated by fluorescence spectroscopy for pyrene used a guest molecule in aqueous medium (ref.[3] and citations in). The gelation of SDC occurs in aqueous solution at the p*H* values close to the physiological ones that require fine tuning of external parameters.[21]

The solubilization of $Mgcr_8Pc$ in micellar SDC solutions was reported by us previously.[11] The process turns possible due to (a) the proximity of Na^+ diameter (1.90 Å) to the cavity size in 15-crown-5-ether (1.7–2.2 Å) and (b) the formation of *guest–host* complexes in micellar solutions of SDC. So, in case of three-deck La complex, the encapsulation of Na^+ ions was confirmed by the broadening of proton resonance signals from methylene groups of the 15-crown-5-fragments fused with the macrocycle and their low-field shifting.[32] The NMR (^{1}H, ^{1}H-^{1}H NOESY) and absorption spectra of $Mgcr_8Pc$ solubilized in aqueous micellar SDS

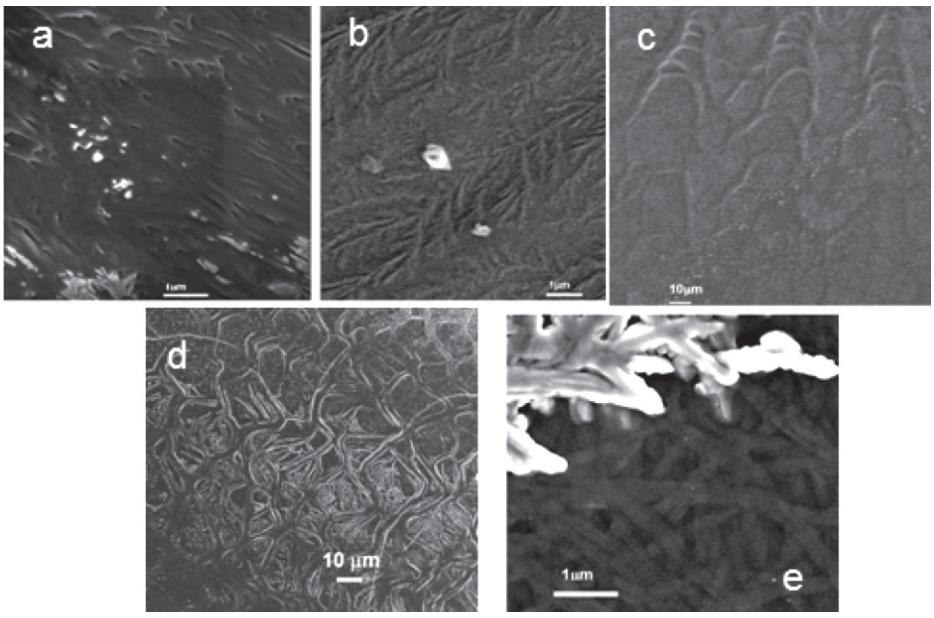

Figure 11. SEM images of $Mgcr_8Pc$/SDC/NaCl xerogel (a) and $Mgcr_8Pc$/SDC/NaCl aerogel without (a–c) and with (d, e) carbon coating.

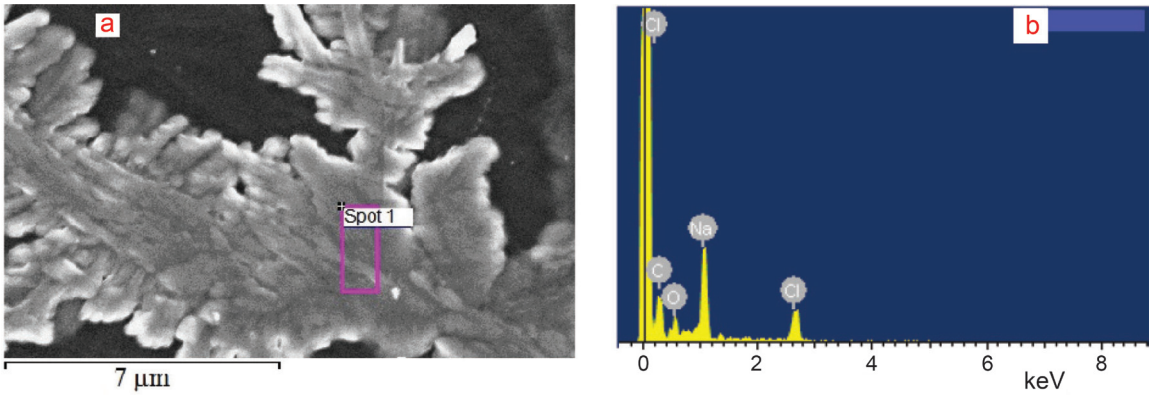

Figure 12. EDX spectrum of $Mgcr_8Pc$/SDC/NaCl aerogel.

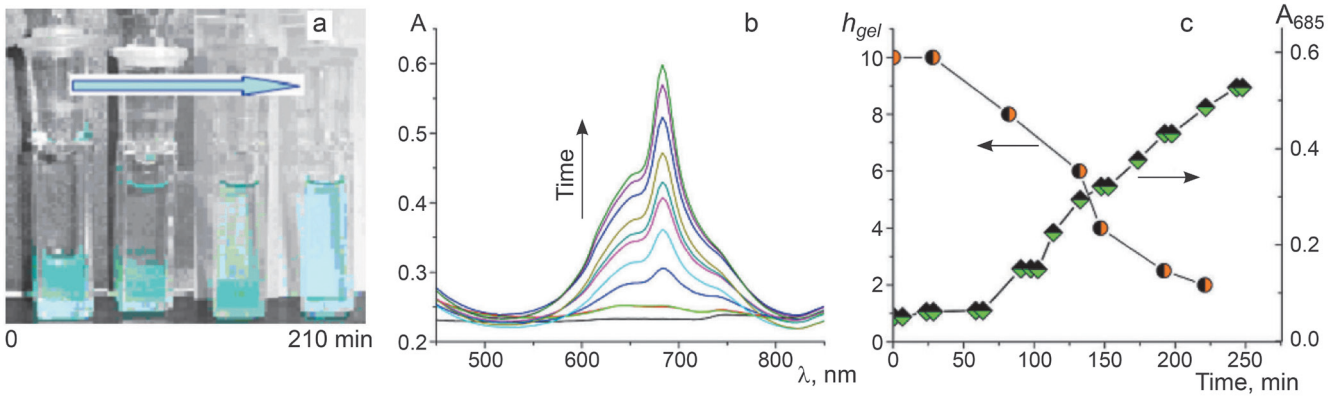

Figure 13. Release of $Zncr_8Pc$ from $Zncr_8Pc$/SDC/lys·HCl/NaCl hydrogel in the presence of lysine. Photos of gel, two-phase system, and $Zncr_8Pc$ solution (a); spectral changes in the aqueous phase obtained in the course of gel dissolution (b); gel height h_{gel} and absorbance A_{685} as a function of time ([lysine]=0.153 M) (c).

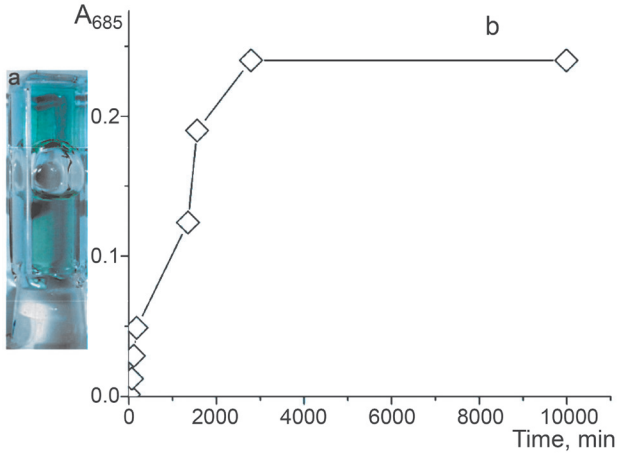

Figure 14. Release of $Zncr_8Pc$ from $Zncr_8Pc$/SDC/lys·HCl/NaCl gel in the absence of lysine. a: the cell turned upside down at some time moment within the ascending part of the plot in Figure 14b, b: the absorbance (A_{685}) of the aqueous solution as a function of time.

solution suggest that the formation of micelle-bound $Mgcr_8Pc$ monomer is possible (*i*) upon synergic complexation of Na^+ ions with crown fragments in $Mgcr_8Pc$, (*ii*) due to electrostatic interaction between the polar $–OSO_3^-$ group and complexed Na^+ ion, and (*iii*) due to the interaction between aromatic protons in $Mgcr_8Pc$ with the protons of aliphatic chain in SDS.[13] The presence of the latter ones is indicative of the $Mgcr_8Pc$ encapsulation into hydrophobic environment in the microheterogeneous SDS medium.

A distinctive feature of the solubilization of crown-containing Pc with sodium deoxycholate is the influence of the ionic force of solution on a molecular state of Pc (largely monomeric); the effect was explained by a decrease in CMC and by the growth of micelles in the presence of NaCl.[11] In the absence of a central metal atom (Mg or Zn), the solubilization of H_2cr_8Pc with bile salts does not result in formation of Pc monomers, in contrast to the microheterogeneous SDS medium.[15] Tentatively, the formation of $Mgcr_8Pc$ aqua complexes favors their solubilization with BS in the presence of physiological NaCl concentrations to yield largely Pc monomers. The formation of mono and di(aqua)complexes of MgPc was reported earlier.[33]

Solubilization of crown-containing phthalocyanines with SDC afforded for their incorporation, as an active component, into SDC-containing hydrogels to yield fluorescing species. The addition of NaCl not only improves the mechanical properties of gel,[25] but also facilitates the monomerization of Pc in the presence of BS.[11] Upon a change in the aggregation state of the system (gel melting), $Mgcr_8Pc$ ($Zncr_8Pc$ or $Mgcr_4Pc$) undergoes transition from

the aggregated to monomeric state; as a result, the fluorescence intensity of $Mgcr_8Pc$ grows.[12] Another way to go about releasing the active agent is a decrease in the strength of SDC/NaCl gel by addition of amino acids with a high hydropathy index.[28] *In vitro* experiments, L-lysine and L-arginine (hydropathy indices –3.9 and –4.5)[34,35] led to the disruption of non-covalent interactions and hence to weakening the mechanical strength of SDC-based supramolecular gel, which resulted in the release of active component, methylene blue,[25] or Pc in our case (see Figures 13 and 14). The release rate can be readily varied. The surface character of formed xero- and aerogels is defined by the type of SDC/NaCl-based aggregates, which agrees with the available literature data.

Conclusions

Thus, in this work we managed to extend the circle of natural surfactants suitable for solubilization of Pc in aqueous media and also explored the behaviour of crown-containing Pc in the process. Phthalocyanine entered the gel as an active component that can be released from the gel under the action of external influences such as heating or the addition of some amino acids. Some basic characteristics of gels and xerogels formed with participation of crown-containing Pc have been presented. No doubt that the influence of Pc on the morphology and parameters of xero- and aerogels deserves further investigation.

Abbreviations

Bile acid salt	BS
Sodium deoxycholate	SDC
Sodium taurodeoxycholate	STDC
Sodium dodecyl sulfate	SDS
Scanning electron microscopy	SEM
Phthalocyanine, crown-containing phthalocyanine	Pc
Lysine hydrochloride	lys·HCl

Acknowledgments. The work was supported by Federal Agency of Scientific Organizations (grant no. 0089-20-14-0036) and Program for Basic Research I.8P. We are also grateful to Yu.V. Baskakova for taking the IR spectra.

Notes and References

1. Bhattacharya S., Samanta S.K. *Chem. Rev*. **2016**, *116*, 11967–12028.
2. Babu S.S., Praveen V.K., Ajayaghosh A. *Chem. Rev*. **2014**, *114*, 1973–2129.
3. Zhang M., Strandman S., Waldron K.C., Zhu X.X. *J. Mater. Chem. B* **2016**, *4*, 7506–7520.
4. Yu G., Yan X., Han C., Huang F. *Chem. Soc. Rev*. **2013**, *42*, 6697–6722.
5. Lauren B.E., Rowan S.J. *Chem. Soc. Rev.* **2012**, *41*, 6089–6102.
6. Svobodová H., Noponen V., Kolehmainen E., Sievänen E. *RSC Adv*. **2012**, *2*, 4985–5007.
7. Maity G.C. *J. Phys. Sci*. **2008**, *12*, 173–186.
8. Weiss R.J. *J. Amer. Chem. Soc*. **2014**, *136*, 7519–7530.
9. Holm R., Mullertz A., Mu H. *Int. J. Pharm*. **2013**, *453*, 44–55.
10. Stojančević M., Pavlović N., Goločorbin-Kon S., Mikov M. *Frontiers in Life Science* **2013**, *7*, 112–122.
11. Gol'dshleger N.F., Lobach A.S., Gak V.Yu., Kalashnikova I.P., Baulin V.E., Tsivadze A.Yu. *Protect. Met. Phys. Chem. Surf.* **2014**, *50*, 599–607.
12. Goldshleger N.F., Gak V.Yu., Lobach A.S., Kalashnikova I.P., Baulin V.E., Tsivadze A.Yu. *Macroheterocycles* **2015**, *8*, 343–350.
13. Goldshleger N.F., Chernyak A.V., Kalashnikova I.P., Baulin V.E., Tsivadze A.Yu. *Russ. J. Gen. Chem.* **2012**, *82*, 927–935.
14. Logacheva N.M., Baulin V.E., Tsivadze A Yu., Basova T.V., Sheludyakova L.A. *Russ. Chem. Bull.* **2008**, *57*, 1467–1476.
15. Gol'dshleger N.F., Baulin V E., Tsivadze A.Yu. *Protect. Met. Phys. Chem. Surf*. **2014**, *50*, 135–172.
16. Bhattarai A., Kumar Shah S., Kumar Yadav A., Adhikari J. *Bibechana* **2013**, *9*, 63–68.
17. *The Bile Acids: Chemistry, Physiology, and Metabolism*: *Vol. 1, Chemistry* (P.P. Nair, D. Kritchevsky, Eds.), New York: Springer Science, **1971**.
18. Hydrogels or alcogels that are dried in air or in vacuum at room temperature are called xerogels. They can retain their original shape but the drying process is often accompanied by sample cracking. When the liquid is extracted in a supercritical state, such materials are called aerogels.
19. Under UV illumination, $Mgcr_8Pc$/SDC/lys·HCl gel exhibited weak fluorescence, which agrees with the predominantly aggregated state of $Mgcr_8Pc$ (see spectrum 1 in Figure 6c).
20. Kasha M., Rawis H.R., El-Bayoumi M.A. *Pure Appl. Chem.* **1965**, *11*, 371–392.
21. Zhang J., Wang H., Li X., Song S., Song A., Hao J. *J. Phys. Chem. B* **2016**, *120*, 6812–6818.
22. Suzuki H., Ogawa M., Hironaka K., Ito K., Sunada H. *Drug Dev. Ind. Pharm.* **2001**, *27*, 943–949.
23. Kumar S., Randhawa J.K. *Colloids Surf. B: Biointerfaces* **2013**, *102*, 562–568.
24. In the card file JCPDS-ASTM, the following reflexes are given for NaCl (PDF card 05-628): d=3.26, 2.82, 1.99, 1.63, 1.41, 1.26, 1.15, and 0.89 Å.
25. Zhang Y., Xin X., Shen J., Tang W., Ren Y., Wang L. *RSC Adv*. **2014**, *4*, 62262–62271.
26. Das S., de Rooy S.L., Jordan A.N., Chandler L., Negulescu I.I., El-Zahab B., Warner I.M. *Langmuir* **2012**, *28*, 757–765.
27. In the presence of lysine, it took 3 h at the concentrations used.
28. The hydropathy index is a number that characterizes the hydrophobicity or hydrophilicity of the side chain in amino acids: the greater its value, the more hydrophobic the amino acid.
29. Lapkina L.A., Gorbunova Y.G., Gil D.O., Ivanov V.K., Konstantinov N.Yu., Tsivadze A.Yu. *J. Porphyrins Phthalocyanines* **2013**, *17*, 564–572.
30. Komissarov A.N., Makarov D.A., Yuzhakova O.A., Savvina L.P., Kuznetsova N.A., Kaliya O.L., Lukyanets E.A., Negrimovsky V.M. *Macroheterocycles* **2012**, *5*, 169–174.
31. Goldshleger N.F., Lobach A.S., Baulin V.E., Tsivadze A.Yu. *Russ. Chem. Rev*. **2017**, *86*, 269–297.
32. Birin K.P., Gorbunova Yu.G., Tsivadze A.Yu. *Protect. Met. Phys. Chem. Surf.* 2011, *47*, 417–423.
33. Janczak J. *Polyhedron* **2010**, *29*, 941–949.
34. Ide M., Maeda Y., Kitano H. *J. Phys. Chem. B* **1997**, *101*, 7022–7026.
35. Kyte J., Doolittle R.F. *J. Mol. Biol*. **1982**, *157*, 105–132.

Received 11.08.2017
Accepted 31.08.2017